9/18/95

CM 1995/Q:12

Theme Session on Intermediate-Scale Physical Processes and their Influence on the Transport and Food Environment of Fish (Q)

Interannual Variability of Mesoscale Eddies and Patchiness of Young Walleye Pollock as Inferred from a Spatially Explicit, Individual-Based Model

Albert J. Hermann[1,2]
Sarah Hinckley[3]
Bernard A. Megrey[3]
Phyllis J. Stabeno[2]

[1]Joint Institute for the Study of the Atmosphere and Ocean
University of Washington, Seattle

[2]NOAA, Pacific Marine Environmental Laboratory
Seattle, Washington

[3]NOAA, National Marine Fisheries Service, Alaska Fisheries Science Center
Seattle, Washington

Corresponding author address: National Oceanic and Atmospheric Administration, Pacific Marine Environmental Laboratory, 7600 Sand Point Way NE, Seattle, WA 98195, hermann@pmel.noaa.gov

INTRODUCTION

The Gulf of Alaska is rich in physical and biological variability, and serves as a nursery for large populations of gadoid fishes. A species of major interest in this area is walleye pollock, *Theragra chalcogramma*. The Fisheries Oceanography Coordinated Investigations (FOCI) research program was initiated in 1984 to investigate how features of the environment affect recruitment of this species (Schumacher and Kendall, 1995; Schumacher and Kendall, 1991; Kendall et al., 1995). Adult pollock spawn in late March to early April at the western end of Shelikof Strait, between Kodiak Island and mainland Alaska (Fig. 1). Eggs are fertilized at depths between 150-200 m, and hatch into larvae after a period of about 2 weeks. These larvae rise to the upper 50 m of the water column and drift in the prevailing currents for the next several weeks (late April - mid-May). Larger larvae undergo diel migrations between 15-50 m. Currents may carry the larvae southwestward along the Alaska Peninsula, or offshore along the shoreward edge of the Shelikof Sea Valley southwest of Shelikof Strait. Only a small portion of the larvae hatched from the spawned eggs survive. By mid-summer, many of the survivors have been advected to juvenile nursery grounds near the Shumagin Islands, ~300 km to the southwest of the spawning site. A central hypothesis of FOCI posits that for successful recruitment, most early juveniles must reach nursery areas along the Alaska Peninsula. Processes occurring during this transport should also be important, e.g. retention in mesoscale eddies. The spatial paths are significantly influenced by the vertical migration of each individual according to its life stage and size (Hinckley et al., 1995). Here, we model the growth and development of individuals, which are in turn affected by the spatial path. Lacking a suitable prey and predator model at present, we focus on temperature as a determinant of feeding and respiration rates. We demonstrate that spatial paths differ dramatically in different years, driven by the interannual variability of the physical forcing, and that even a model with no spatial variability in prey can yield patchiness in both 1) spatial density of larvae and 2) length of larvae.

Five years are considered in this report: 1978, 1987, 1988, 1989, and 1991. These span a wide range of meteorological conditions (winds, runoff) and recruitment success. These attributes are summarized in Table 1. The years analyzed may be considered as natural experiments involving two fundamentally different "treatments": runoff and winds (Fig. 2). We focus most of our presentation on: a dry year with strong winds (1978), a wet

year with average winds (1987), a wet, windy year (1988), a dry, calm year (1989). These experiments are discussed in more detail in Hermann et al. (1995).

METHODS

We combine a three-dimensional, nonlinear, eddy-resolving hydrodynamic model of Shelikof Strait and the surrounding area with a probabilistic, individual-based life stage model. Wind and runoff drive the hydrodynamic model, which generates velocity, salinity, and temperature fields. The individual-based model tracks representative fish throughout the study region, using velocity, salinity and temperature fields generated by the hydrodynamic model (Fig. 3). A total of 1600 individuals were "spawned" in a rectangular pattern near the exit of the Strait (Fig. 1). Each individual is followed from spawning through egg, yolk-sac larva, feeding larva, and juvenile life stages, with mortality, feeding, and growth modeled appropriately at each stage.

Details of the physical model design, implementation, and sensitivity analysis are given in Hermann and Stabeno (1995). A detailed comparison of hindcast versus measured velocity fields has been presented in Stabeno and Hermann (1995). This comparison established that the model replicates observed mean current patterns and drogued drifter tracks. Mesoscale features (e.g. eddies) were produced at appropriate rates and spatial scales. Differences between model and data were largely attributable to differences in the timing of eddy formation.

The detailed structure of the biological model is described in Hinckley *et al.* (1995). In the feeding larva and juvenile stages, appropriate Q10 factors are applied to determine mean daily consumption and metabolic rates as a function of temperature. A random deviate from a normal distribution is then used for daily consumption of an individual. Changes in individual depths are driven by the behavioral response to the modeled physical environment, and vertical advection by the circulation field (Fig. 4).

RESULTS

Salinity and velocity patterns

As a result of the interannual variability in wind and runoff, the different years exhibit significantly different salinity and velocity fields. The mean velocity field for 1978 and 1988 exhibits a strong flux through the Strait, trapped against the coastal boundary and flowing out the exit of the sea valley, to join with the Alaskan Stream (Fig. 5). In 1987,

the mean flow is seen to meander significantly in the center of the sea valley; this reflects the repeated formation of vortex pairs in that area. In 1989, the mean flow is significantly weaker than in any of the other years, with a weak anticyclonic pattern at the head of the sea valley. Velocity fields were further analyzed for mean eddy kinetic energy (i.e. variance of the velocity through time) during the simulation. The year of strongest winds and strong runoff (1988) exhibited the highest values of eddy kinetic energy. Year 1987 was next, reflecting the prevalence of mesoscale eddies driven by the powerful runoff that year. Year 1978 exhibited weaker values than 1987, with 1989 (a year of weak winds and runoff) exhibiting the lowest values overall.

Larval density patterns

We compare the concentration of modeled individuals at day 142 with the measured concentration of larvae during day 135-150 (May 15-31) for 1987, 1988 and 1989 (Fig. 6). The aggregated field data were gleaned from earlier FOCI studies of larval advection (e.g. Hinckley et al., 1991). In late May of 1987, larvae were found concentrated to the west and south of Kodiak Island, with a large number centered near the coastline. Modeled individuals at this time appear focused at the same latitude, but primarily in the sea valley, and trapped in the cyclonic eddy feature there (see below). In 1989, two intense maxima of larval concentration were observed upstream of the 1987 locations. Smaller concentrations were found near the exit of the sea valley, between Chirikof and the Semidi Islands. The model reproduced this pattern extremely well. Most significantly, the enhanced concentrations of larvae found in the field in 1989, relative to 1987, were faithfully reproduced by the model.

Individual positions and lengths

Individual positions are plotted with length indicated by shading (Fig. 7). Barotropic streamfunction is superimposed to indicate the velocity field. As in the larval density maps, day 142 exhibits large differences among years.

The 1978 run yielded smooth flow through most of the Strait, with meandering and eddy-like structures further along in the sea valley. The 1987 run produced a prominent matched pair of counter rotating eddies in the upper sea valley, with other eddy features present in the Strait. The 1988 run produced a single prominent eddy at the head of the sea valley, while the 1989 run produced no prominent eddy features in the sea valley or shelf area.

For the 1989 run, individuals clustered near their release point. In the 1987 run, they were carried somewhat farther to the southwest, and a large number were entrained into an eddy pair in the center of the sea valley on that date. Few were carried as far as the Shumagin Islands. Conversely, in 1978 and 1988, many of the individuals were swept into the Alaskan Stream and past the Shumagin Islands by day 142. In 1978, large numbers collected on the shallow shelf northeast of the Shumagin Islands, due to strong shelfward flows prior to day 142. Note the general tendency in the stronger forcing years (1978, 1987, 1988) for individuals to shear out along the streamlines of flow.

When eddy activity is weak (e.g. 1989), there is a natural tendency for the larger individuals to be located further downstream of the release point. When eddy activity is strong (e.g. 1987), individuals of a particular size class can become trapped in closed circulation features. Note in particular how the individuals trapped in the cyclonic member of the 1987 eddy pair tended to be greater in length than the rest of the population, while those trapped in the anticyclonic member tended to be smaller. Measured lengths for 1987 reveal spatial patchiness at similar scales, with patches of both short and long individuals (Fig. 8).

By day 262, when all individuals had reached the juvenile life stage, few individuals remained in the sea valley (Fig. 9). In the 1987 run, individuals were uniformly dispersed on the shelf area to the northeast of the Shumagins. In other years, the distribution of modeled individuals was much patchier; note especially the strong aggregation of individuals along the coastline in 1978 and 1989.

Spatial statistics

Two useful statistics for quantifying advection and patchiness of individuals among years are 1) the number of individuals remaining on the shelf between Kodiak Island and the Shumagins on any given date, and 2) Lloyd's index of patchiness for individuals remaining in that area.

Prior to day 120, the 1988 run exhibited the largest number of retained larvae (Fig. 10a). The 1989 run yielded the largest number of retained larvae on day 135 and subsequently, whereas the 1988 run yielded the least beyond that day. Year 1987 yielded high retention of larvae through day 175, after which large numbers were lost from the area.

Lloyd's index of patchiness (Lloyd, 1967) is defined as:

$$P = 1 + (\sigma^2 - m)/m$$

where m is the mean density of larvae in the area and σ^2 is the variance in that area. We calculate this statistic by grouping the modeled larvae into 0.2° longitude by 0.1° latitude bins for the shelf area between the southwestern edge of Kodiak Island and the northeastern edge of the Shumagins.

The calm, dry year (1989) yielded an especially patchy distribution of larvae. For 1978 patchiness generally increased beyond the early larval stage. In 1987, patchiness achieved a maximum in the middle of the run (days 175-225) but ultimately dropped to lower values than all other years on day 262 (P ~ 3.0). Year 1988 achieved maximum patchiness around day 160 (P ~ 5.0), with low values thereafter. An average time series of P for all years matches observed trends in P derived from multi-year data in the region, with values of P ~ 5.0 for both model and data at day 142 (Stabeno et al., 1995).

DISCUSSION

It appears that eddies are capable of both enhancing and destroying the patchiness of young pollock in the study area, depending on the time of year. In the early part of some years, eddies were observed to trap young individuals in the model, as has been observed in data from this area (Schumacher *et al.*, 1993). Such trapping yields a patchy distribution of larvae, and in some cases a patchy distribution of lengths. However, note that larvae outside of the eddies will be subjected to a greater degree of horizontal mixing when such mesoscale features are abundant. Stated another way, high values of eddy kinetic energy yield high values of eddy diffusivity. We suggest that the large amount of eddy kinetic energy in 1987 mixed the juvenile population after the initial patches of larvae had disintegrated. This led ultimately to the uniform spatial distribution at day 262 of 1987, as compared with the other years (Fig. 14b).

AKNOWLEDGMENTS

Computational resources were supplied by the Arctic Region Supercomputing Center. Analysis and graphing of model results was performed using FERRET, developed by Steve Hankin and Dr. Ed Harrison at PMEL.

REFERENCES

Hermann, A. J., and Stabeno, P. J. (1995) An eddy-resolving circulation model for the western Gulf of Alaska shelf. I. Model development and sensitivity analyses. *J. Geophys. Res.*, in press.

Hermann, A. J., Hinckley, S., Megrey, B. A., and Stabeno, P. J. (1995) Interannual Variability of the Early Life History of Walleye Pollock near Shelikof Strait as Inferred from a Spatially Explicit, Individual-Based Model. *Fish. Oceanogr.*, in review.

Hinckley, S., Bailey, K. M., Picquelle, S. J., Schumacher, J. D., and Stabeno, P. J. (1991) Transport, distribution, and abundance of larval and juvenile walleye pollock (*Theragra chalcogramma*) in the western Gulf of Alaska. *Can. J. Fish Aquat. Sci.* **48:** 91–98.

Hinckley, S., Hermann, A. J., and Megrey, B. A. (1995) Development of a spatially explicit, individual-based model of marine fish early life history. *Mar. Ecol. Prog. Ser.*, in review.

Kendall, A. W., Jr., Schumacher, J. D., and Kim, S. (1995) Walleye pollock recruitment in Shelikof Strait: applied fisheries oceanography. *Fish. Oceanogr.*, in review.

Lloyd, M. (1967) Mean crowding. *J. Anim. Ecol.* **36:** 1-30.

Megrey, B. A., Bograd, S. J., Rugen, W. C., Hollowed, A. B., Stabeno, P. J., Macklin, S. A., Schumacher, J. D., and Ingraham, W. J., Jr. (1995b) An exploratory analysis of associations between biotic and abiotic factors and year-class strength of Gulf of Alaska walleye pollock (Theragra chalcogramma), p. 227-243. *In* Beamish, R. J. (ed.), Climate change and northern fish populations. *Can. Spec. Publ. Fish. Aquat. Sci.* **121.**

Royer, T. C. (1982) Coastal freshwater discharge in the northeast Pacific. *J. Geophys. Res.* **87:** 2017–2021.

Schumacher, J. D., and Kendall, A. W., Jr. (1991) Some interactions between young walleye pollock and their environment in the western Gulf of Alaska. *CalCOFI Rep.* **32:** 22-40.

Schumacher, J. D., and Kendall, A. W., Jr. (1995) Fisheries oceanography: Walleye pollock in Alaskan waters. *American Geophysical Union U. S. National Report,* in press .

Schumacher, J. D., Stabeno, P. J., and Bograd, S. J. (1993) Characteristics of an eddy over a continental shelf: Shelikof Strait, Alaska. *J. Geophys. Res.* **98:** 8395-8404.

Stabeno, P. J., and Hermann, A. J. (1995) An eddy-resolving circulation model for the western Gulf of Alaska shelf. II. Comparison of results to oceanographic observations. *J. Geophys. Res.*, in press.

Stabeno, P. J., Schumacher, J. D., Bailey, K. M., Brodeur, R. D., and Cokelet, E. D. (1995) Observed patches of walleye pollock eggs and larvae in Shelikof Strait, Alaska: their characteristics, formation and persistence. *Fish. Oceanogr.*, in review.

List of Figures

Fig. 1 Overview of geography and circulation in the northwestern Gulf of Alaska, with early life history of the population of walleye pollock (*Theragra chalcogramma*) near Shelikof Strait. Arrows indicate typical paths of pre-spawning adults, larvae, and early juvenile stages. Isobaths are shown in meters. Inset map shows regional circulation. Hatched area indicates region of spawning for 1600 individuals (40 x 40 grid) used in biological model. Dashed line indicates boundary of finely resolved (~4 km spacing) domain of circulation model.

Fig. 2 Scatterplot of southwestward wind stress versus runoff for the five years. Values are averages for the period January-May of each year. Runoff values are from Royer (1982 and personal communication), and represent total input of freshwater along the Gulf of Alaska coastline upstream of Shelikof Strait.

Fig. 3 Summary of coupling between hydrodynamic and biological models. Wind and runoff time series drive the hydrodynamic model (Seminspectral Primitive Equation Model; SPEM), which writes out daily filtered velocity (U), salinity (S) and temperature (T) fields. The Individual Based Model (IBM) uses these daily fields to track individuals through space (with self-directed vertical motions added), yielding time series of position (X), temperature (T), salinity (S), length (size), weight, and stage for each individual.

Fig. 4 Time series of depth for a typical individual in the coupled model. Time axis is marked by life stage (egg, yolk-sac larva [YSL], feeding larva [FDL]), and is not to scale. Random vertical migration is added to the FDL stage in the model, beyond the point where diel migration begins (when FDL > 6mm stadard length).

Fig. 5 Comparison of average modeled velocity fields for day 60-269 at 40 m depth for 1978, 1987, 1988, and 1989. Key indicates length of 0.75 m s^{-1} velocity vector.

Fig. 6 a) Density of individuals in the individual based model runs (normalized to larval density, number per 10 m^2) on day 142 (May 22) for two years: 1987 and 1989. Only nonzero density areas are shaded. b) Measured larval density (in number per 10 m^2) for all individuals collected during May 15-31 in each of the two years. Shaded, contoured areas indicate the spatial extent of the collected data.

Fig. 7 Individual-based model results for day 142 (May 22). Individual positions are greyscale-coded by the length (mm) of the individual. Contours of barotropic streamfunction (in 10^6 m^3 s^{-1}) are superimposed to indicated circulation field. Contour interval for streamfunction is 0.1 for values between -1.0 and 1.0, and 1.0 for values less than -1.0.

Fig. 8 Closeup of length distribution near Shelikof Strait: a) results from model; b) data from larval surveys. Lengths are in mm. Barotropic streamfunction is superimposed as in Fig. 7.

Fig. 9 Individual-based model results for day 262 (Sep 22).

Fig. 10 Statistics of individuals within the sea valley and shelf area (excluding Shelikof Strait), as a function of time for the five years modeled: a) number of individuals on the shelf between Kodiak Island and the Shumagin Islands; b) Lloyd's patchiness index for individuals within the same area.

Table 1. Interannual variability in runoff, winds, and recruitment. Recruitment estimates are from Megrey *et al.* (1995).

year	month	runoff	winds	recruitment of year class
1978	Mar	moderate	moderate	strong
	Apr	moderate	weak	
	May	moderate	strong	
1987	Mar	strong	strong	weak
	Apr	moderate	moderate	
	May	strong	moderate	
1988	Mar	strong	strong	moderate
	Apr	strong	strong	
	May	weak	moderate	
1989	Mar	weak	moderate	weak
	Apr	weak	weak	
	May	weak	weak	
1991	Mar	moderate	weak	weak
	Apr	moderate	strong	
	May	strong	strong	

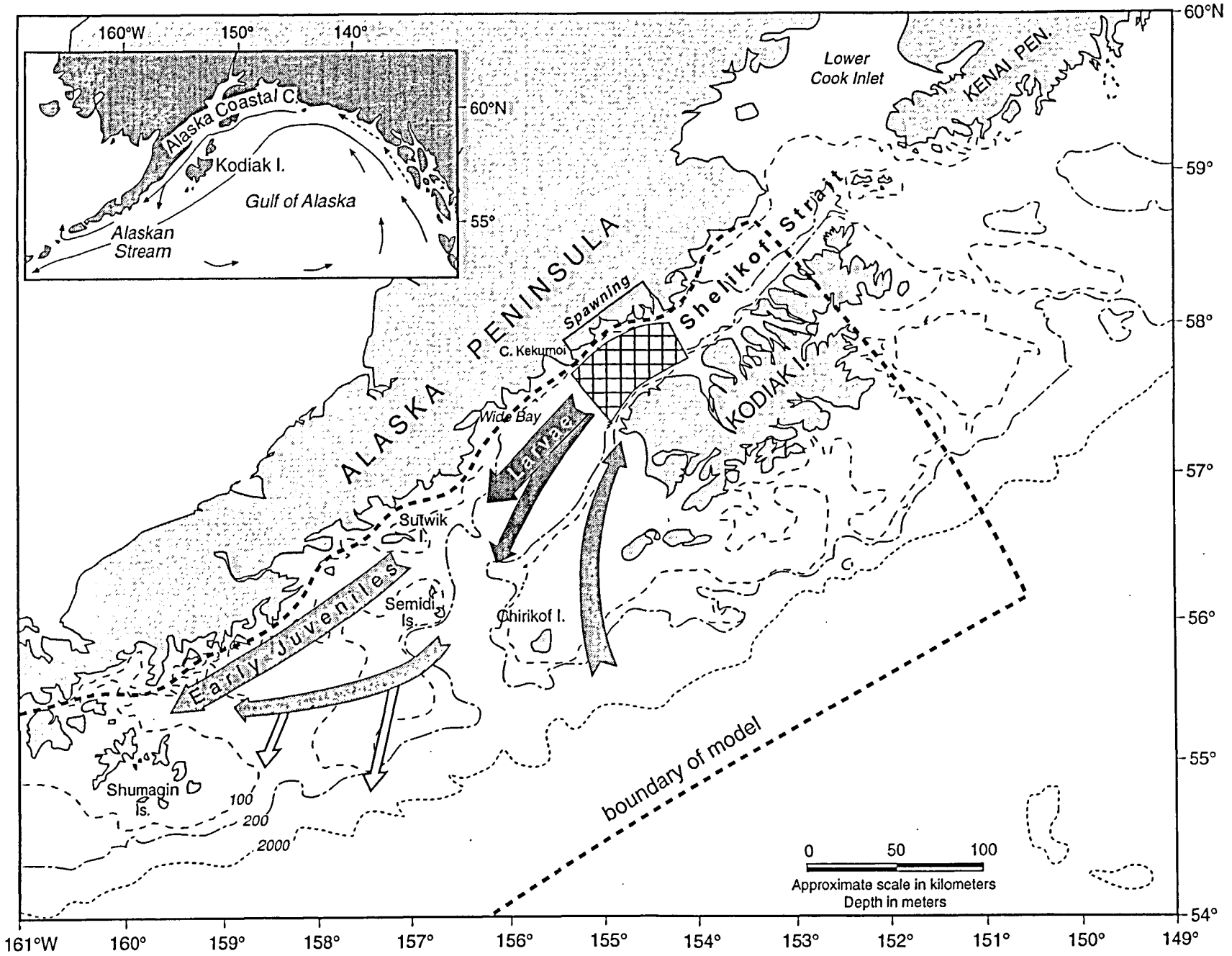
160°W
150°
140°
60°N
55°
Alaska Coastal C.
Kodiak I.
Gulf of Alaska
Alaskan Stream
Lower Cook Inlet
KENAI PEN.
ALASKA PENINSULA
Spawning
C. Kekumoi
Shelikof Strait
KODIAK I.
Wide Bay
Larvae
Sutwik I.
Semidi Is.
Chirikof I.
Early Juveniles
Shumagin Is.
100
200
2000
boundary of model
0 50 100
Approximate scale in kilometers
Depth in meters
60°N
59°
58°
57°
56°
55°
54°
161°W
160°
159°
158°
157°
156°
155°
154°
153°
152°
151°
150°
149°

Fig. 1

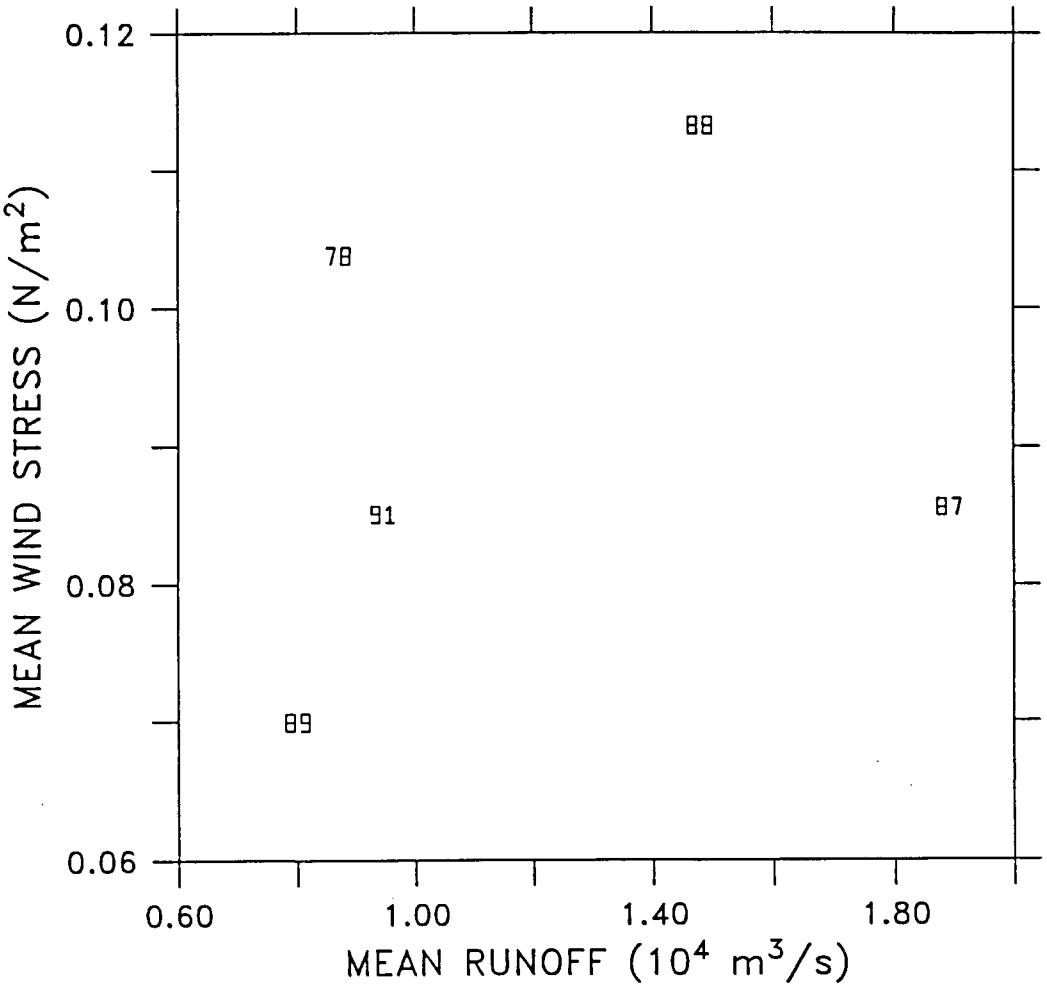
0.12
0.10
0.08
0.06
MEAN WIND STRESS (N/m²)
88
78
91
87
89
0.60
1.00
1.40
1.80
MEAN RUNOFF (10⁴ m³/s)

Fig. 2

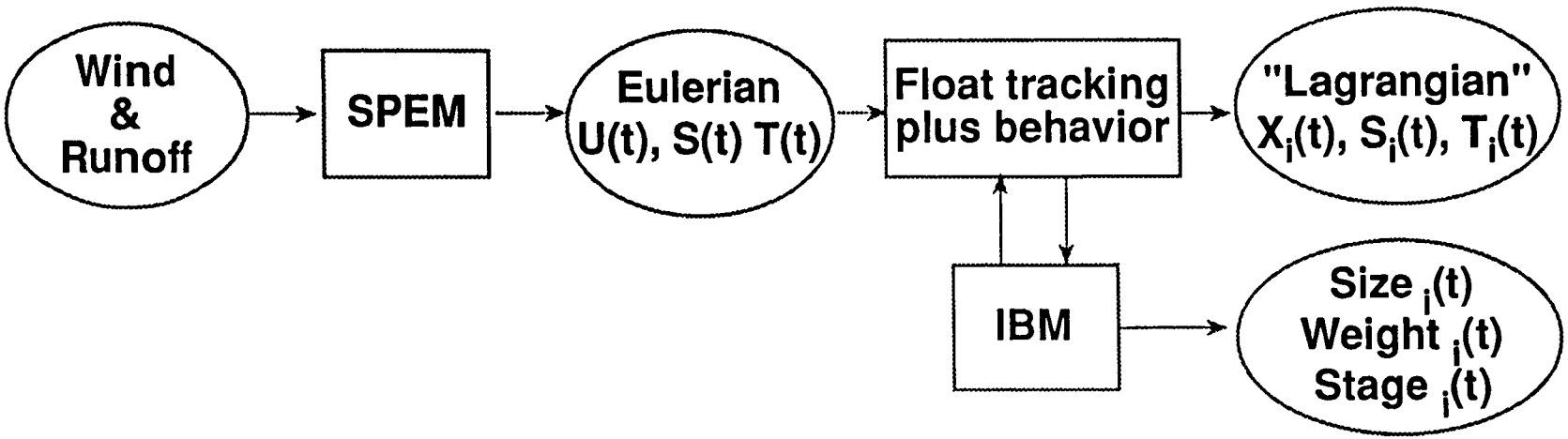
Wind
&
Runoff
SPEM
Eulerian
U(t), S(t) T(t)
Float tracking
plus behavior
"Lagrangian"
$X_i(t)$, $S_i(t)$, $T_i(t)$
IBM
Size $_i(t)$
Weight $_i(t)$
Stage $_i(t)$

Fig. 3

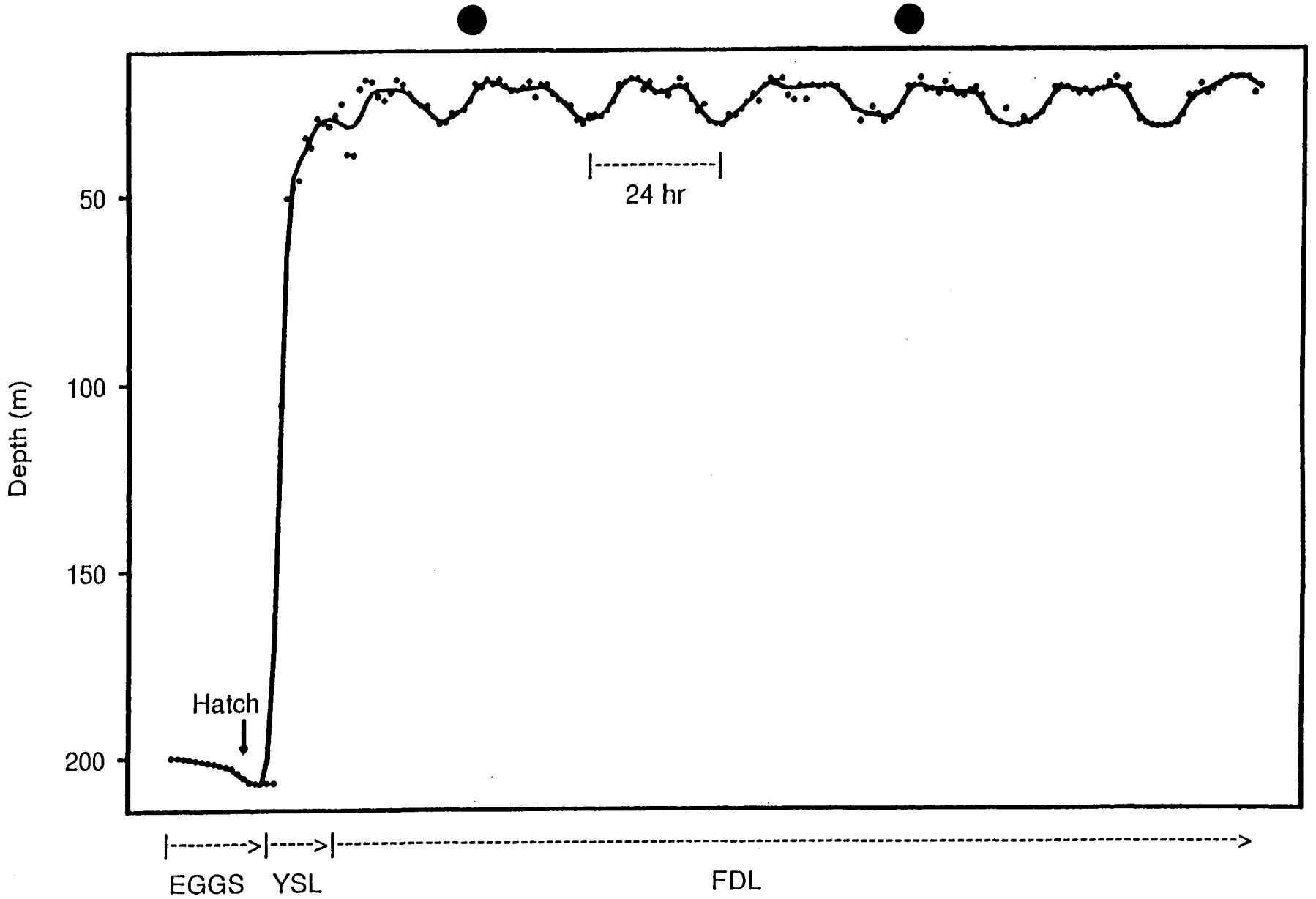

YSL = Yolk-sac larvae

FDL = Feeding larvae

Note: Diel migration starts when FDL are >6 mm SL

Fig. 4

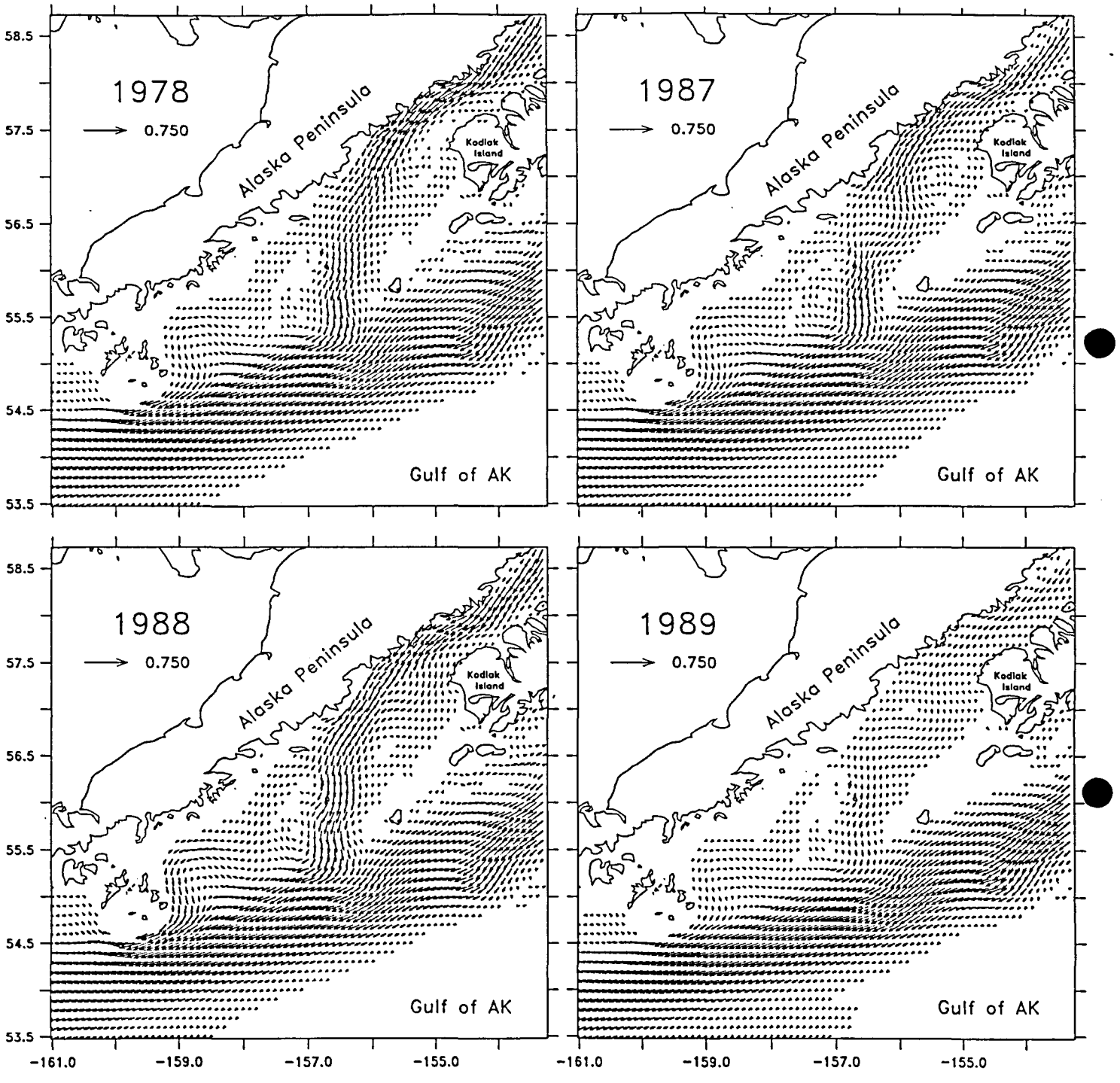
1978
0.750
Alaska Peninsula
Kodiak Island
Gulf of AK
1987
0.750
Alaska Peninsula
Kodiak Island
Gulf of AK
1988
0.750
Alaska Peninsula
Kodiak Island
Gulf of AK
1989
0.750
Alaska Peninsula
Kodiak Island
Gulf of AK
58.5
57.5
56.5
55.5
54.5
53.5
-161.0
-159.0
-157.0
-155.0

Fig. 5

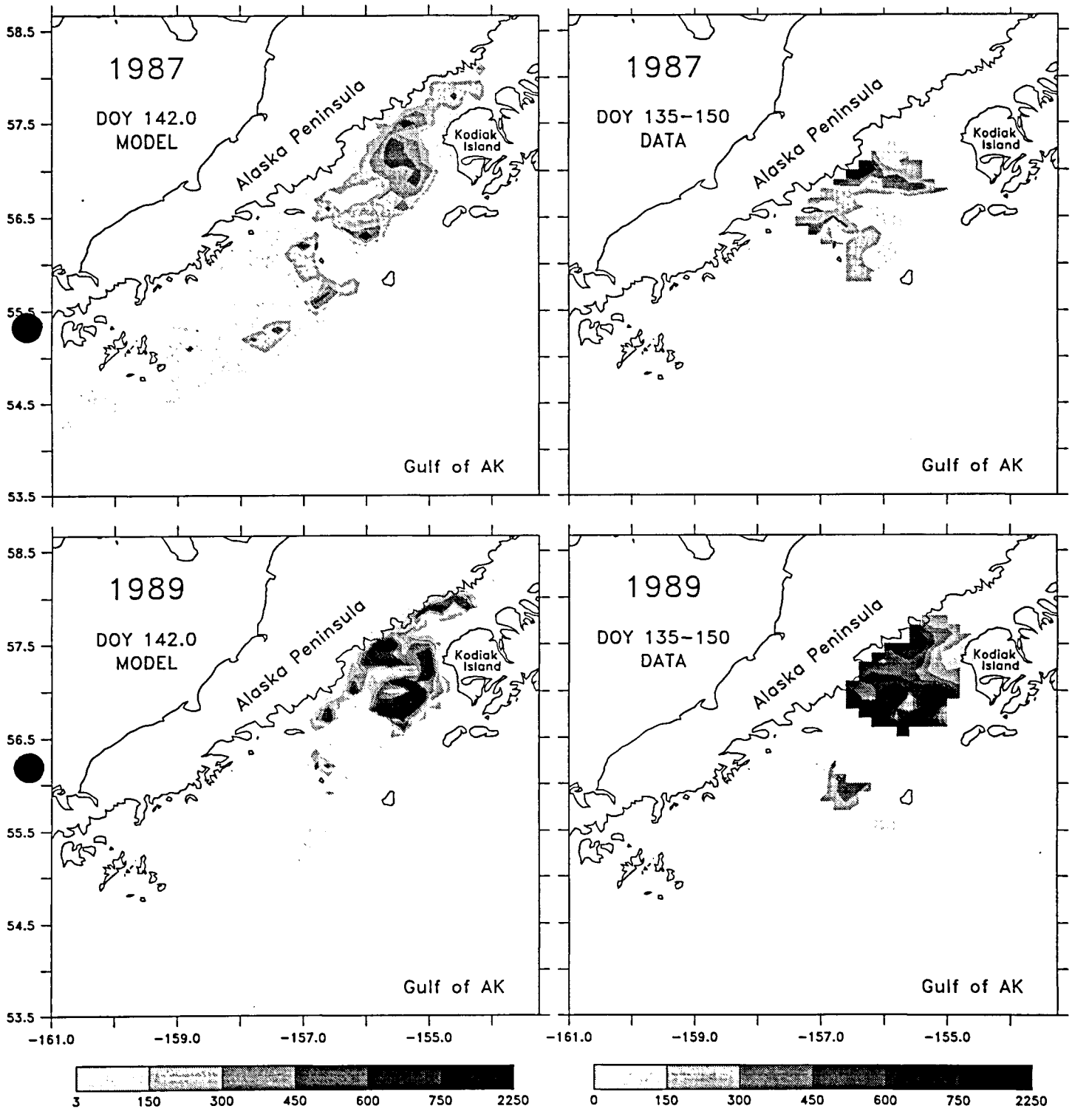
1987
DOY 142.0
MODEL
1987
DOY 135-150
DATA
1989
DOY 142.0
MODEL
1989
DOY 135-150
DATA
Alaska Peninsula
Kodiak Island
Gulf of AK
58.5
57.5
56.5
55.5
54.5
53.5
-161.0
-159.0
-157.0
-155.0
3
150
300
450
600
750
2250
0
150
300
450
600
750
2250

(a) (b)

Fig. 6

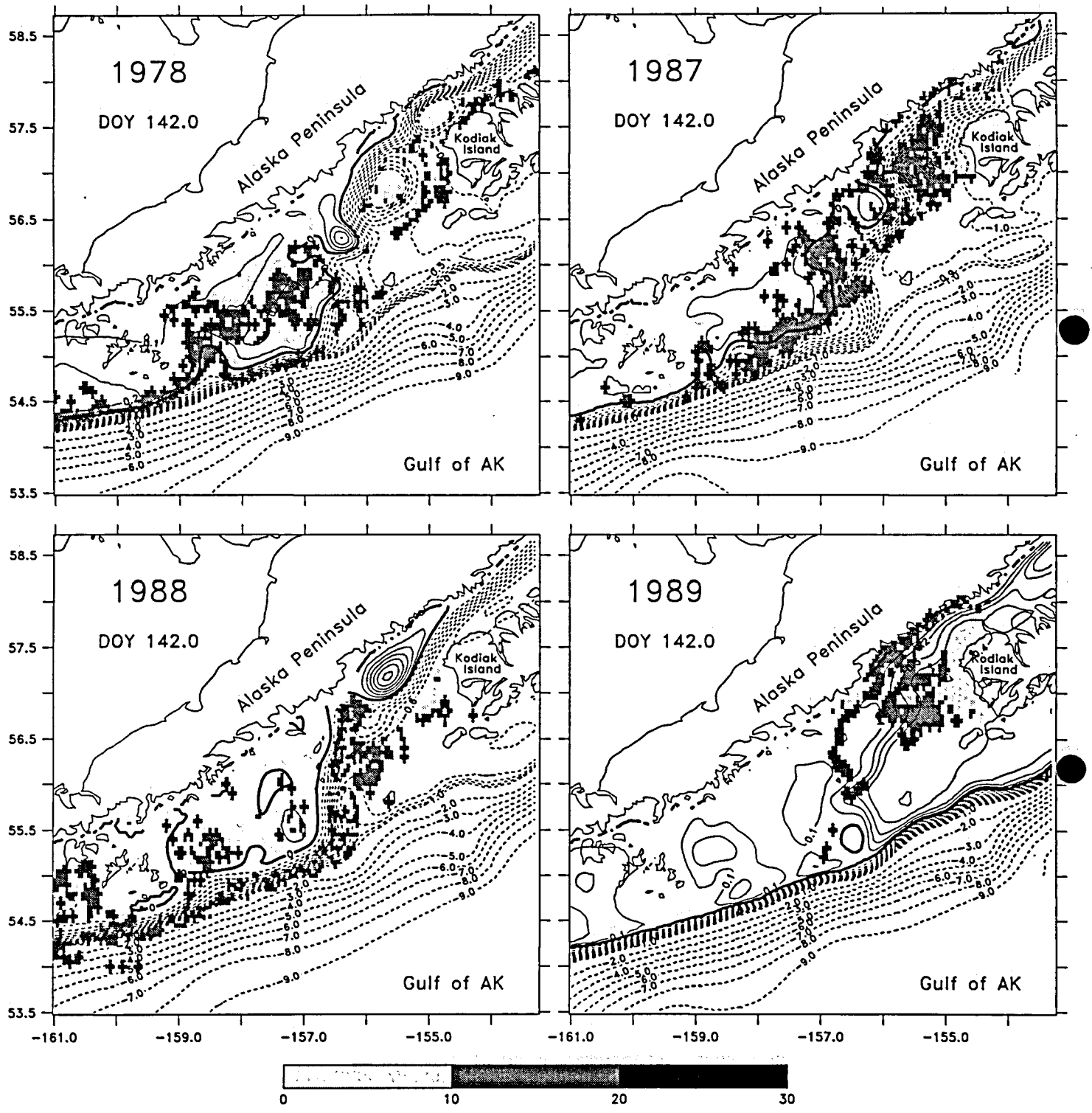
1978
DOY 142.0
1987
DOY 142.0
1988
DOY 142.0
1989
DOY 142.0
Alaska Peninsula
Kodiak Island
Gulf of AK
58.5
57.5
56.5
55.5
54.5
53.5
-161.0
-159.0
-157.0
-155.0
0
10
20
30

Fig. 7

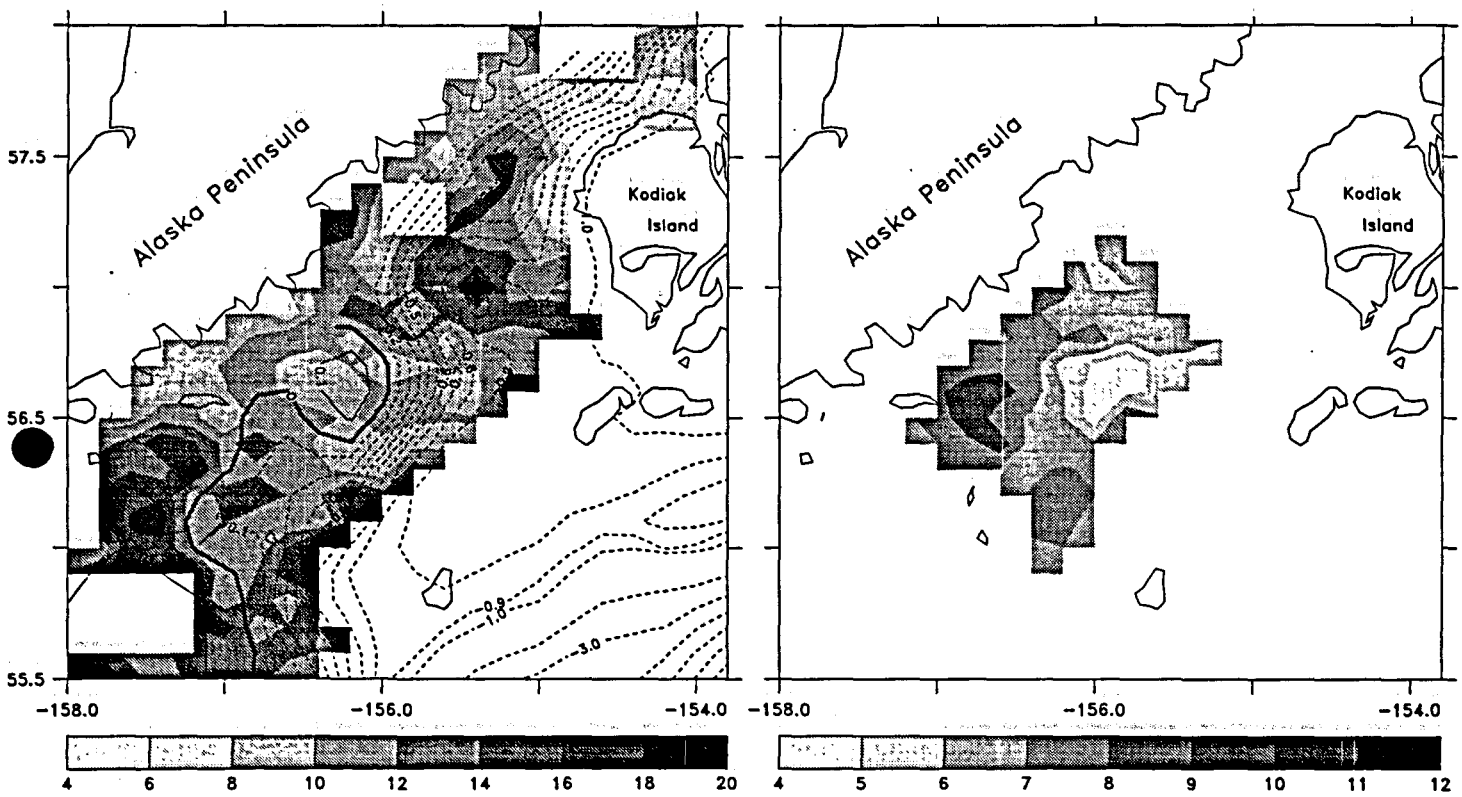
Alaska Peninsula
Kodiak
Island
57.5
56.5
55.5
-158.0
-156.0
-154.0
0.0
0.5
1.0
3.0
4 6 8 10 12 14 16 18 20
4 5 6 7 8 9 10 11 12

(a) (b)

Fig. 8

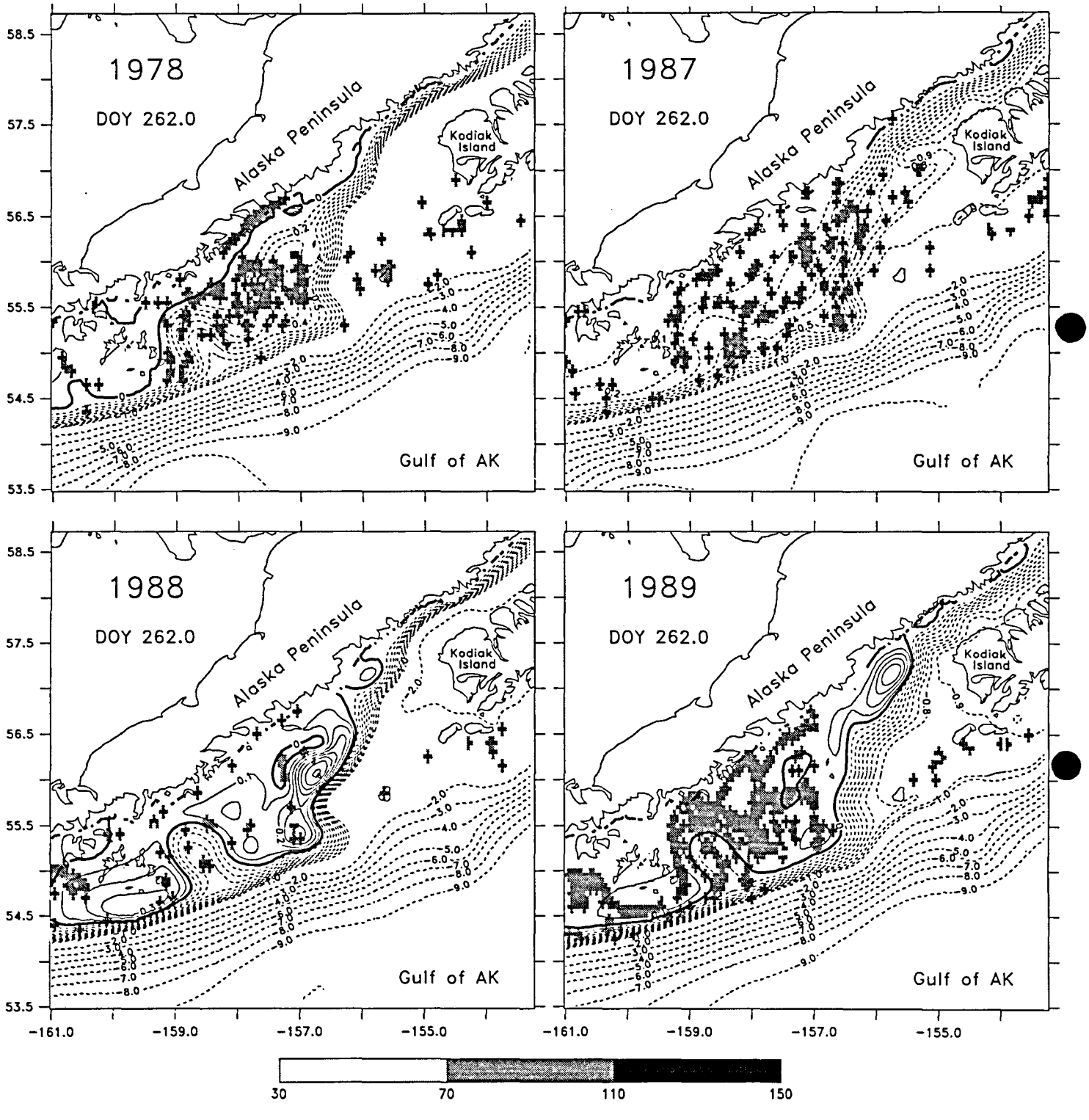
1978
DOY 262.0
1987
DOY 262.0
1988
DOY 262.0
1989
DOY 262.0
Alaska Peninsula
Kodiak Island
Gulf of AK
58.5
57.5
56.5
55.5
54.5
53.5
-161.0
-159.0
-157.0
-155.0
30
70
110
150

Fig. 9

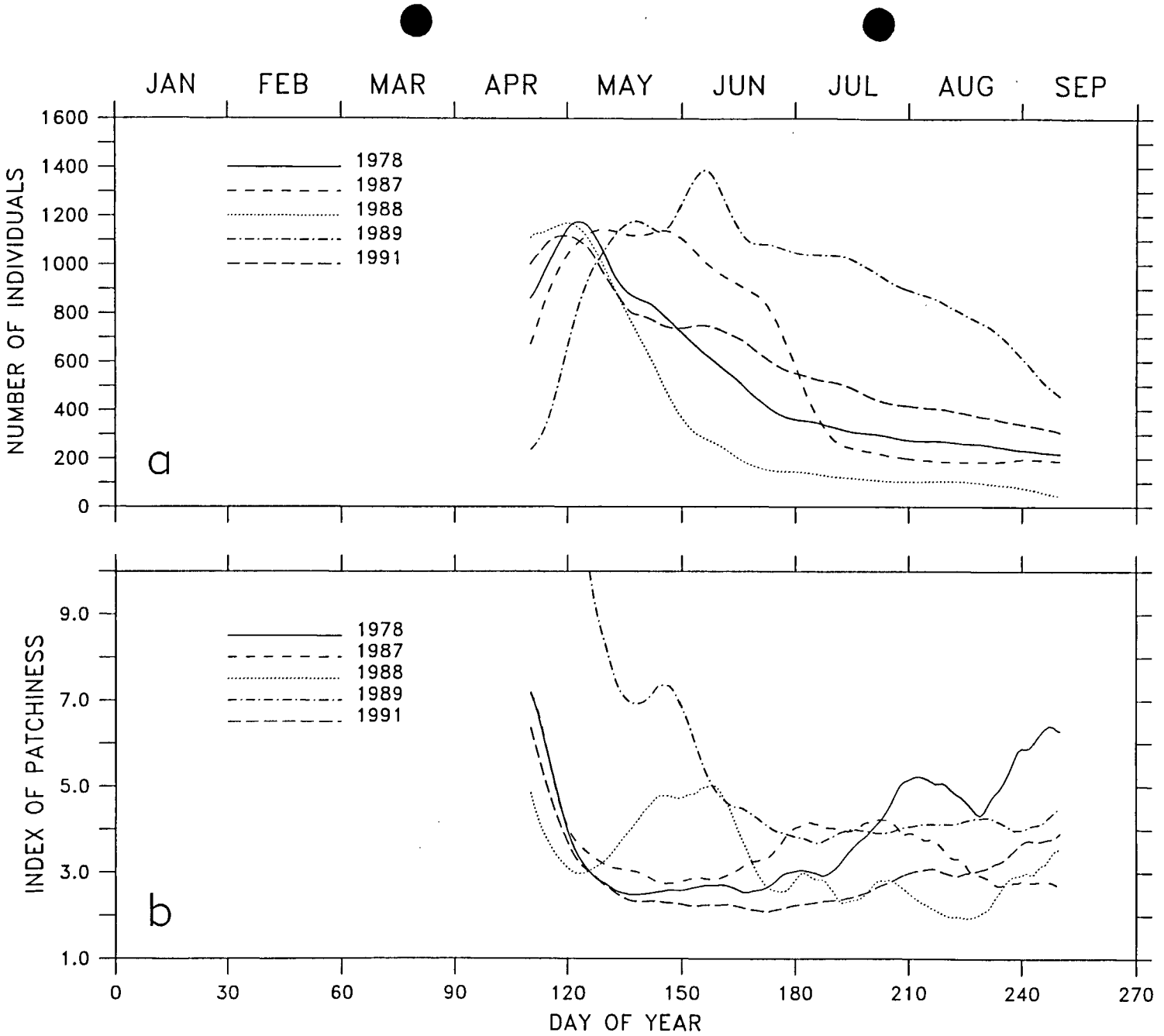
JAN
FEB
MAR
APR
MAY
JUN
JUL
AUG
SEP
NUMBER OF INDIVIDUALS
1600
1400
1200
1000
800
600
400
200
0
1978
1987
1988
1989
1991
a
INDEX OF PATCHINESS
9.0
7.0
5.0
3.0
1.0
b
0
30
60
90
120
150
180
210
240
270
DAY OF YEAR

Fig. 10